Current Topics in Electrochemistry
Vol. 21, 2019

Review

Review of the electrochemical deposition of an aluminum layer using aprotic solvents, old and new solvents, additives, and new technologies

Touya Kujime, Fuma Ando, Takao Gunji and Futoshi Matsumoto*

Department of Materials and Life Chemistry, Kanagawa University, 3-27-1, Rokkakubashi, Kanagawa-ku, Yokohama, Kanagawa 221-8686, Japan.

ABSTRACT

This review paper examines old and new solvents, additives and technologies for the electrochemical deposition of aluminum (Al), which has properties of low density, high heat conductivity and electron conductivity, and high corrosion resistance. The advantages and disadvantages of each material and technology especially with respect to their application in Al deposition baths are summarized. In addition, the application of Al deposition in the areas of nanotechnology and energy conversion is also reviewed.

KEYWORDS: aluminum, electrochemical deposition, aprotic solvent, ionic liquid, eutectic solvent.

1. Introduction

Aluminum (Al) metal has properties of low density (2.7 $g \cdot cm^{-3}$), high heat conductivity (237 $Wm^{-1} \cdot K^{-1}$) and electron conductivity (37.7 x 10^{-6} $S \cdot m^{-1}$), and high corrosion resistance and is used in various areas; for example, aluminum foil is used in daily life, and aluminum is used in the parts and bodies of cars and railroad vehicles [1]. The density of Al is much lower than that of iron (Fe, 7.9 $g \cdot cm^{-3}$) and copper (Cu, 4.5 $g \cdot cm^{-3}$) [2]. Therefore, Al metal has been used as a substitute for Fe and Cu to reduce the weight of the product. Al easily forms an aluminum oxide layer on its surface under air, resulting in high corrosion resistance [3]. In addition, Al does not have a toxic effect on the human body and environment [4].

Al deposition on some substrates is used to impart the properties of Al to the surface of the substrates [5]. The deposition of Al, which is mined largely from the earth's crust, will supersede the deposition of Zn [6] which has general applicability and widely used as a coating metal because of its low price and because there is less chance of resource depletion. The main method of Al deposition presently is the hot dip metal coating method [7]. However, a high temperature, large apparatus and heat-resistant substrates (on which the coating metal is deposited) are needed. Therefore, the price of the substrates on which Al coating is deposited by hot dip metal coating is high.

To decrease the price of Al-coated substrates electrochemical deposition of Al at room temperature has been examined. The electrochemical deposition of Al using aqueous solutions cannot be performed because the standard redox potential of Al/Al^{3+} is -1.67 V (*vs.* normal hydrogen electrode (NHE)), which is lower than that of $H_2/2H^+$ (0 V), and therefore, hydrogen evolution occurs preferentially instead of Al deposition [8]. Electrochemical Al deposition was examined using anhydrous electrolytes [9-11], inorganic molten salts [12, 13] and organic molten salts, that is, ionic liquids (ILs) [14-18] that do not contain protons in the solvents.

*Corresponding author: fmatsumoto@kanagawa-u.ac.jp

As a representative bath for the electrochemical deposition of Al, an IL of aluminum chloride ($AlCl_3$)-di-alkylimidazolium chlorides (DAIC, for example, 1-ethyl-3-methyl-imidazolium chloride (EMIC)) has been widely used [19, 20]. Thick [21] and/or high-brightness layers [22, 23] of Al on some substrates could be formed from the ILs at room temperature. However, $AlCl_3$-DAIC ILs have several disadvantages, including low air and water resistance [15]. $AlCl_3$-alkylimidazolium-tetrafluoroborate and -hexafluorophosphate ILs produce hydrogen fluoride (HF) by the slow hydrolysis of BF_4^- and PF_6^- anions with water [24]. Therefore, this bath cannot be used under an atmosphere containing moisture and cannot be applied in mass production. Recently, many attempts have been made to overcome the weakness of the IL. The weakness of the IL is being eliminated by new ideas, for example, the protection of the IL using hydrocarbon layers that protect against air and water [23, 25] and the development of new solvents, such as water-stable ILs [26-28] and eutectic solvents [29-31]. In this paper, various projects to overcome the weakness of the IL will be reviewed. Then, the characteristics of the project will be mentioned. In addition, to increase the areas of application of Al surface coating, the formation of high brightness Al, electroless deposition of Al, nanotechnology of Al deposition and application of Al deposition in batteries will also be reviewed.

2. Performance of the $AlCl_3$-DAIC bath

During the period when electrochemical deposition of Al was invented, it was studied using high-temperature molten salts, such as NaF-AlF_3 [32], NaCl-KCl-AlX_3 (X = Br or Cl) [33] and NaCl-$AlCl_3$ [34]. However, the molten salts need a high temperature above 150 °C and generate corrosive gases. These negative points become large hurdles for the industrialization of electrochemical plating of Al. As a measure to overcome the disadvantage of high-temperature molten salts, room-temperature molten salts and ILs that are liquids below 100 °C were developed. Many types of room-temperature molten salts and ILs have been synthesized [30, 35, 36] and applied in the electrochemical deposition of Al [10, 37, 38]. Among the room-temperature molten salts and ILs, $AlCl_3$-DAIC was the most frequently examined ionic liquid because of its low melting point, low vapor pressure and high chemical stability. It is classified as part of the first generation of ILs. In particular, in an acidic bath (50 mol% < $AlCl_3$) of $AlCl_3$-EMIC, the $Al_2Cl_7^-$ ion is an electrochemically active species for Al deposition (eq. 1), and nucleation of Al occurs frequently during the electrochemical deposition in the bath, resulting in the formation of a flat Al layer.

$$4Al_2Cl_7^- + 3\ e^- \rightarrow Al + 7AlCl_4^- \quad (1)$$

The electrochemically deposited Al layers have attractive properties, such as high coulombic efficiency [39], high corrosion resistance [40] and crystallographic orientations of Al deposits as mentioned below [41]. The electrodeposition efficiency was over 90%, although the percentage strongly depended on the kind of bath [39, 42]. To form Al layers with high corrosion resistance properties, an Al layer with high density [39], and adhesiveness [39] with some substrates should be deposited. The dense Al layers were formed by changing the current density and electrochemical deposition modes such as potentiostatic polarization [43], galvanostatic pulse polarization [44], monopolar current pulse polarization [39] and bipolar current pulse polarization [39]. Figure 1 shows cyclic voltammograms for Al deposition from $AlCl_3$-1-(2-methoxyethyl)-3-methylimidazolium chloride [45]. In the cathodic branch, a nucleation loop, which indicates initial nucleation and growth, occurred with a significant overpotential. The nucleation loop can be observed in cyclic voltammograms of Al deposition. Peaks for the reversible reduction ($Al^{3+} \rightarrow Al$) and its reverse reaction ($Al \rightarrow Al^{3+}$) can be observed. In the inset of Figure 1 (cathodic potential sweep was reversed before the bulk deposition of Al occurred), three cathodic and four anodic peaks can be observed. Three cathodic peaks of c_1 and c_2 and corresponding reduction peaks a_1 and a_2 correspond to the underpotential deposition process. At peaks c_3 and a_3, the formation of the 3D Al cluster and its reverse reaction occur in the overpotential deposition region. The peaks c_4 and a_4 were recorded during the bulk deposition of Al. These behaviors could be observed during Al deposition. The deposition process of Al was analyzed with current–time

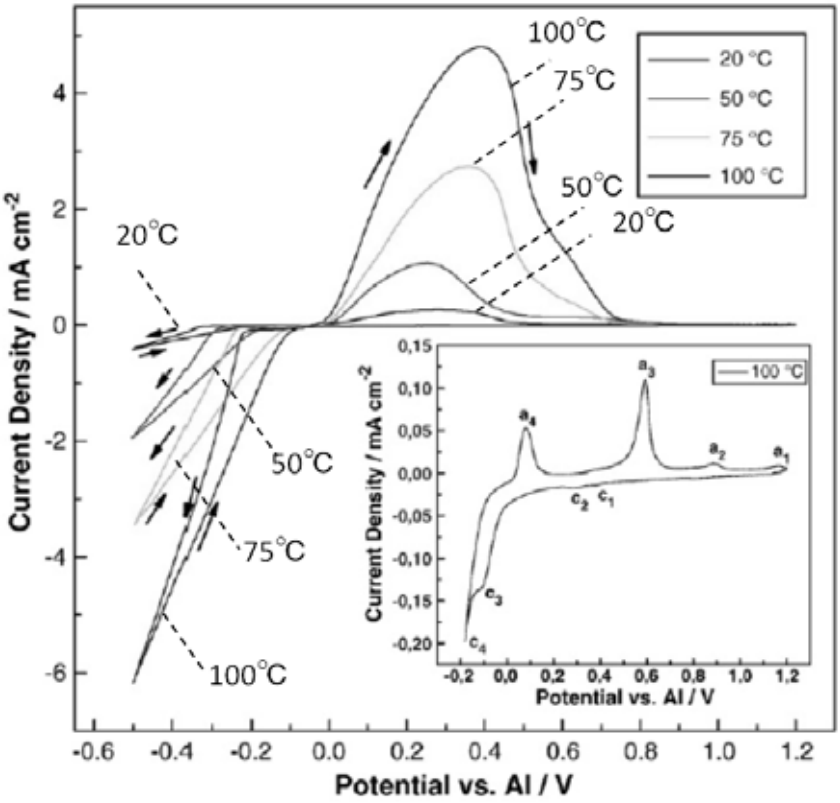

Figure 1. Cyclic voltammograms obtained for Al deposition in $AlCl_3$-1-(2-methoxyethyl)-3-methylimidazolium chloride (60/40 mol%) at different temperatures at a potential scan rate of 10 $mV \cdot s^{-1}$. Inset: cyclic voltammogram measured at 100 °C showing the cathodic processes preceding Al bulk deposition. Reprinted from Electrochem. Commun., 12, Abedin, S. Z. E., Giridhar, P., Schwab, P. and Endres, F., Electrodeposition of nanocrystalline aluminium from a chloroaluminate ionic liquid, 1084-1086, Copyright (2010), with permission from Elsevier.

transient curves obtained in potential-step chronoamperometric experiments. From the current-time transient curves, instantaneous nucleation and progressive nucleation of Al were distinguished at each experimental condition, for example, because the behavior depends on the material of electrode used in Al deposition [16, 46]. To determine the nucleation and growth of Al deposition, the chronoamperometric data were analyzed using plots of (i/i_{max}) *vs.* (t/t_{max}), where i is the current at any time t and i_{max} is the maximum current at time t_{max} (Figure 2) [16, 46]. In Figure 2, the Al deposition from the $AlCl_3$-urea solvent was controlled by a pure 3D instantaneous nucleation mechanism. The addition of toluene to the solvent changed the deposition mechanism. The electrochemical deposition of Al was examined using many substrates. Among them, copper [42, 47, 48], Al [42, 43], platinum [39, 49], steel [49], glassy carbon [50] and W [43, 44] substrates were often used. Proper selection of the substrates improved the adhesiveness of the deposited Al layer to the substrates [43, 44]. In addition, nanocrystalline deposits of Al for the formation of dense Al layers could be achieved by the proper selection of imidazolium cations in IL baths which were composed of imidazolium cations and aluminum chloride anions. The imidazolium cations adsorbed were decomposed electrochemically on the electrode surface during Al deposition [51]. The products formed *via* the cathodic decomposition of the imidazolium cation during Al deposition inhibited the crystal growth of Al deposits, resulting in a dense Al layer. Therefore, the proper selection of imidazolium cations is very important for the formation of dense Al layers. The crystallographic orientations of Al deposits could be changed using current densities and additives.

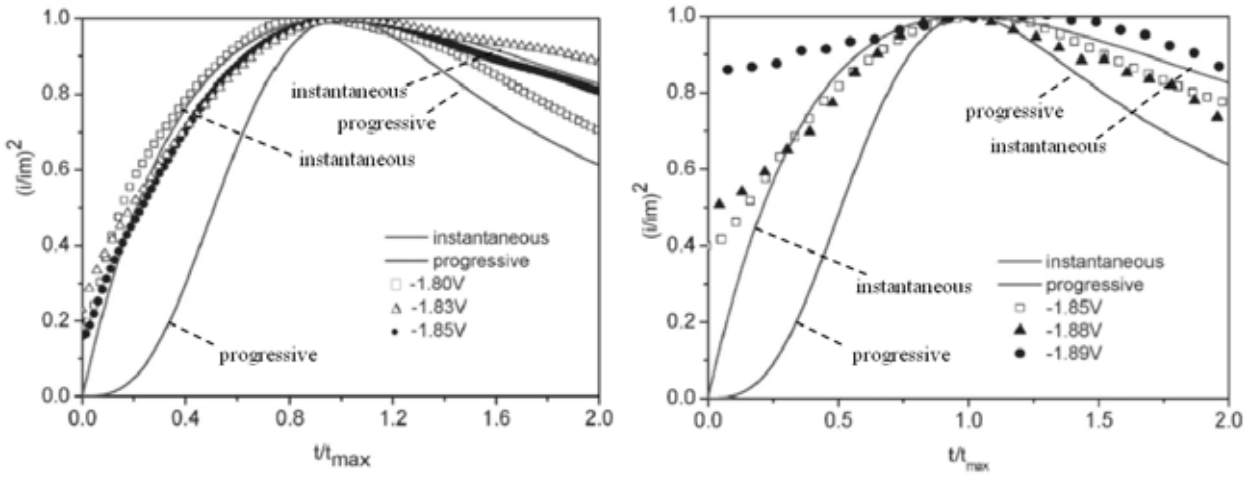

Figure 2. Chronoamperometric current vs. time curves recorded on GC at different potentials for neat 1:1 $AlCl_3$: urea and with 33 v% toluene. Reproduced from Ref. 16 with permission from the PCCP Owner Societies.

For example, the intensity of the (200) plane increased, and the intensity of the (111) plane decreased with increasing current density in the case of $AlCl_3$–1-butyl-3-methyl-imidazolium chloride [50]. It has been reported that cosolvents added to ionic liquids as additives also affect the crystallographic orientations and morphology of Al deposits [52-54, 24]. The reason for these changes was attributed to the change of the speciation from $Al_2Cl_7^-$ to $AlCl_4^-$ for Al deposition. Changes in the equilibrium between $Al_2Cl_7^-$ and $AlCl_4^-$ occurred *via* the addition of a cosolvent to the $AlCl_3$-DAIC bath and $AlCl_4^-$ was formed as the main species in the bath. The addition of the cosolvent accelerates the underpotential deposition of $AlCl_4^-$ onto substrate surfaces, resulting in the change of crystallographic orientations and morphology of Al deposits [55]. Similar to metal deposition using aqueous baths, the electrochemical deposition of Al in the $AlCl_3$-DAIC bath can also form a dense layer by changing the current density and by adding additives to the baths and can easily produce functional layers of Al on various types of substrates.

3. Next generation of Al deposition baths

$AlCl_3$-DAIC baths exhibited high performance for electrochemical Al deposition with respect to coulombic efficiency of deposition and adhesiveness of the Al layer to the substrates. However, these baths have not been applied in mass production because the baths have weak performance with air and water and are corrosive. ILs with resistance to air and water, and noncorrosive properties should be developed in the future [56]. As the second-generation ILs, water- and air-stable ILs have been synthesized using hydrophilic anions [57] such as tetrafluoroborate [58, 59], trifluoromethylsulfonate [59, 60], bis(trifluoromethylsulfonyl)imide [26, 28, 59], tris(trifluoromethylsulfonyl)amide [61, 62] and dicyanamide [63] and cations of alkylpyrrolidinium and alkylimidazolium. Among them, 1-butyl-1-mathylpyrrolidinimu-trifluoromethyl-sulfonate [60], 1-butyl-1-methylpyrrolidinium-bis(trifluoromethylsulfonyl)amide [61], N-methyl-N-alkylpyrrolidinium-dicyanamide [63] and imidazolium-, pyridinium- and guanidinium [64]-perfluoro-3-oxa-4,5-dichloro-pentan-sulphonate [65, 66] ILs with $AlCl_3$ have been used for Al deposition. The number of studies on Al deposition using hydrophobic ILs is low because these ILs cannot perfectly overcome the problem of low resistance against water and air. As an alternate idea, the application of a hydrophobic layer as a protection layer for moisture-sensitive ILs has been proposed. The floating layer of decane which is a nonpolar solvent and does not dissolve in water covers the ILs and can block the contact of ILs with moisture from the air and water. The smooth, mirror-like Al layer from the n-decane/IL bath could be prepared under ambient conditions [16, 23, 25].

To improve the moisture resistance of the bath for Al deposition, third-generation ILs composed of cationic complexes of Al^{3+} ions containing neutral ligands and anionic complexes of Al have been developed. These solutions are called eutectic solvents [30, 67]. When compared with conventional ILs, the specific property of these new solutions is that these solutions contain cationic complexes of Al ions. In conventional ILs, the anionic species $AlCl_4^-$ and $Al_2Cl_7^-$ exist in the solutions. The anionic species containing Al ions transfer to the cathode against the electric field when Al deposition occurs on the cathode substrates. In contrast, the cationic complexes in the eutectic solvents are electrically attracted to the cathode. Therefore, the mechanism of Al deposition in eutectic solvents is different from that in conventional ILs [16]. In addition, the Al^{3+} ions surrounded by neutral ligands might be stable under high-moisture conditions [68]. Urea [16, 69], acetamide [70], ethylene carbonate (EC) [68], dipropyl sulfide [71], substituted pyridine [72], 1-butylpyrrolidine [73], dimethylsulfone [74] and 1,3-dimethyl-2-imidazolidinone [75] have been used as neutral ligands to $AlCl_3$ in the process of Al deposition. According to the following reaction, the cationic and anionic Al species are formed in the solution when $AlCl_3$ and neutral ligands are mixed.

$$x\ AlCl_3 + y\ ligand \leftrightarrow [Al_{x-1}Cl_{3x-4}(ligand)_y]^+ + AlCl_4^- \quad (2)$$

The structure of $[Al_{x-1}Cl_{3x-4}(ligand)_y]^+$ was characterized by mass, Raman, IR and UV-vis spectroscopies, IR and ^{27}Al NMR [68, 76]. For example, in the case of EC [68], Al^{3+} ions are surrounded by the octahedral configuration of four EC molecules and two Cl^- ions with O atoms having double bonding in the EC molecules as coordination points.

The following electrochemical reduction of $[Al_{x-1}Cl_{3x-4}(ligand)_y]^+$ was suggested by Shi [68] in the case of EC ligands:

$$2\ [AlCl_2(EC)_n]^+ + 3e^- \rightarrow Al + [AlCl_4]^- + 2n\ EC \quad (3)$$

When $[AlCl_2(EC)_n]^+$ is reduced at cathode surfaces, EC molecules will be released, and the $[AlCl_4]^-$ produced will be transferred to the anode. It was confirmed that the deposition mechanism of Al could be regarded as instantaneous nucleation under diffusion control and that nanocrystalline Al deposits and a bright surface of Al layers could be formed [16, 69]. ILs composed of $AlCl_3$, neutral ligands and hydrophobic anions, such as trifluoromethanesulfonate and bis(trifluoromethanesulfonyl)-imide, have also been developed and applied in Al deposition [77]. The fact that these ILs have the property of water resistance was confirmed by Dai and coworkers [72]. They compared cyclic voltammograms obtained from $AlCl_3$-EMIC and $AlCl_3$-4-propylpyridine ILs at a molar ratio of 1.3:1 for Al deposition under air containing moisture without protective gas (Figure 3). Although the cyclic voltammograms obtained with $AlCl_3$-EMIC IL exhibited high degradation of reduction and oxidation current densities for Al deposition/stripping reactions, the reduction/oxidation current densities for Al in the $AlCl_3$-4-propylpyridine IL could maintain reaction activity even under moisture, indicating the water resistance of the $AlCl_3$-4-propylpyridine IL. Finally, after 70 min, cyclic voltammograms for $AlCl_3$-4-propylpyridine IL exhibited a much higher reduction/oxidation current when compared with those of the $AlCl_3$-EMIC IL, indicating the advantage of the $AlCl_3$-4-propylpyridine IL under moisture.

Recently, various types of quasi solvents for Al deposition were developed to replace the conventional and recent ILs, which are generally expensive and viscous and have uncertain influences on the environment [78, 79]. As the first quasi solvent, imidazolium iodide ILs containing monomethoxy-terminated poly(ethylene glycol) and n-alkyl groups (PEGylated ILs) were synthesized [80], and PEGylated ILs and KCl salt were used as the solvents to dissolve $AlCl_3$. The PEGylated ILs-KCl-$AlCl_3$ exhibited negligible volatility, low viscosity (approximately 50 mPa·s), intrinsic conductivity, and wide electrochemical window (>2.5 V) for Al deposition [81]. The Al deposition using this solvent could achieve high purity of Al deposits and high adhesive property of Al layers onto substrates even at low overpotential. PEGs with low molecular weight (<800 $g \cdot mol^{-1}$) have properties including low cost, low melting point, negligible vapor pressure, reduced toxicity, high thermal and chemical stability, recyclability, and easy degradability. Therefore, PEGylated ILs will become a promising solvent for electrochemical applications. In the case of the second quasi

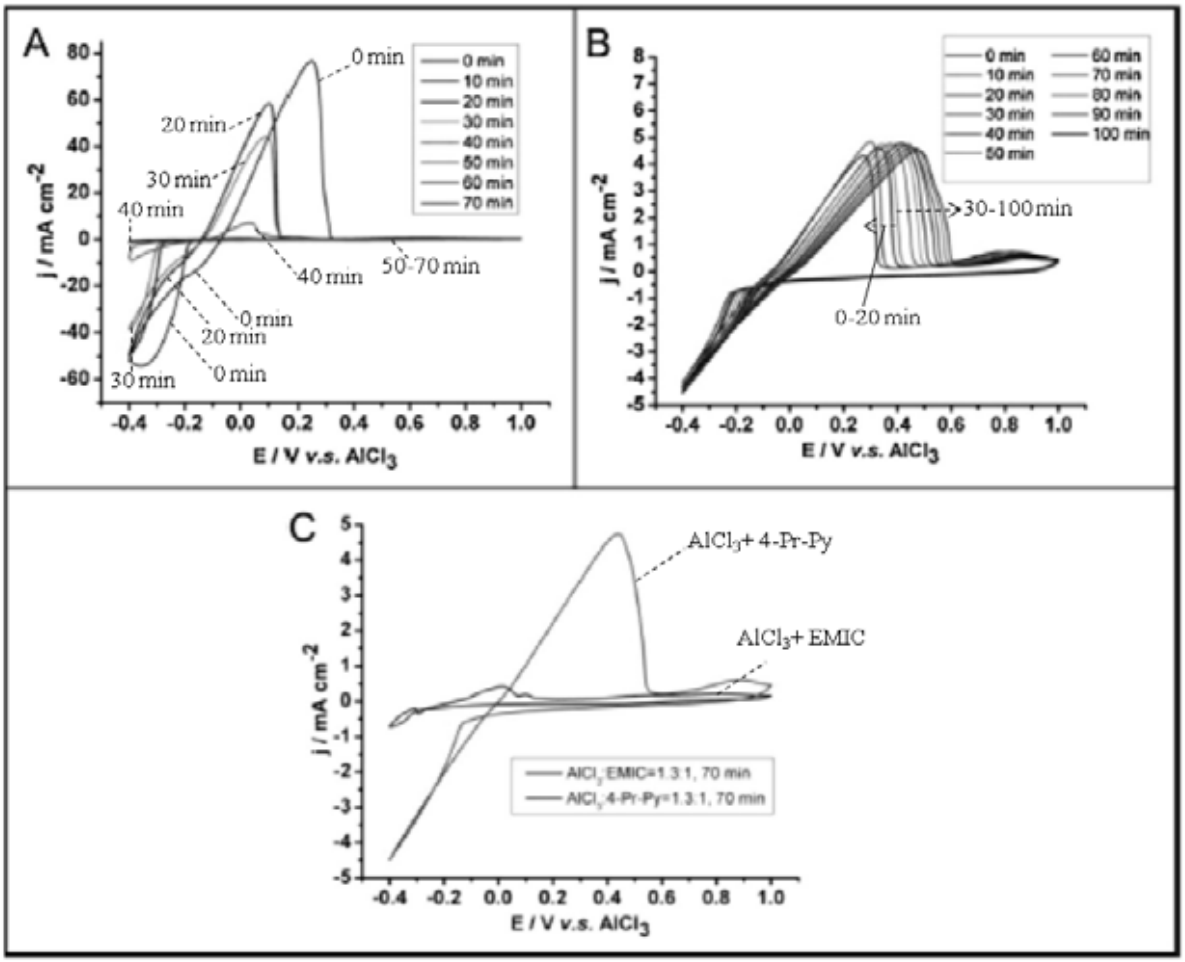

Figure 3. Cyclic voltammograms obtained with (A, C) $AlCl_3$-EMIC and (B,C)$AlCl_3$-4-propylpyridine ILs at a molar ratio of 1.3:1 with Pt working electrodes at a potential scan rate of 100 $mV \cdot s^{-1}$. Reprinted from Electrochim. Acta, 160, Fang, Y., Yoshii, K., Jiang, X., Sun, X.-G., Tusda, T., Mehio, N. and Dai, S. An $AlCl_3$ based ionic liquid with a neutral substituted pyridine ligand for electrochemical deposition of aluminum, 82-88, Copyright (2015), with permission from Elsevier.

solvent, γ-Al_2O_3 was dispersed in the solvent consisting of an organic base and thiourea. The Al layer could be electrochemically formed with the solvent [82]. On the other hand, α-Al_2O_3 could not be dissolved/dispersed in the quasi solvent. The interaction between γ-Al_2O_3 and thiourea contribute to the dissolution/dispersion of γ-Al_2O_3. Not only coordinate bonding (Al···S−C) but also hydrogen bonding (O···H−N) existed in the complexes formed by organic base, thiourea and γ-Al_2O_3.

4. Formation of high-brightness Al surface

Recently, the electrochemical deposition of bright Al films has been reported [83, 84], *i.e.*, films that possess high reflectance values ranging from 70 to 80% in the visible light region. If high-brightness Al film formation can be achieved using electrochemical deposition, Al films would be applicable to a wide range of decorative coatings and optoelectronic materials. The improvement of the brightness of the electrodeposited surface by adding some additives to the baths was examined frequently [85], for example, thiourea in the electrodeposition of copper from an acidic sulphate bath [86] and glycerol, mannitol and sorbitol in the electrodeposition of nickel from a Watts bath [87]. As additives for Al deposition, organic compounds of nicotinic acid and methyl nicotinate

[83, 88], nicotinamide [89], 4-pyridinecarboxylic acid hydrazide [48], polyethylene amines [90] and Span-80, Span-85 and TX-100 [84], 1,10-phenanthroline [91], and inorganic metal salts of LiCl [84], $LaCl_3$ [84] and $ZrCl_4$ [92] were examined. Figure 4 (A-F) shows the micrographs of the Al film surfaces obtained by the electrodeposition of Al in the EMIC/$AlCl_3$/toluene

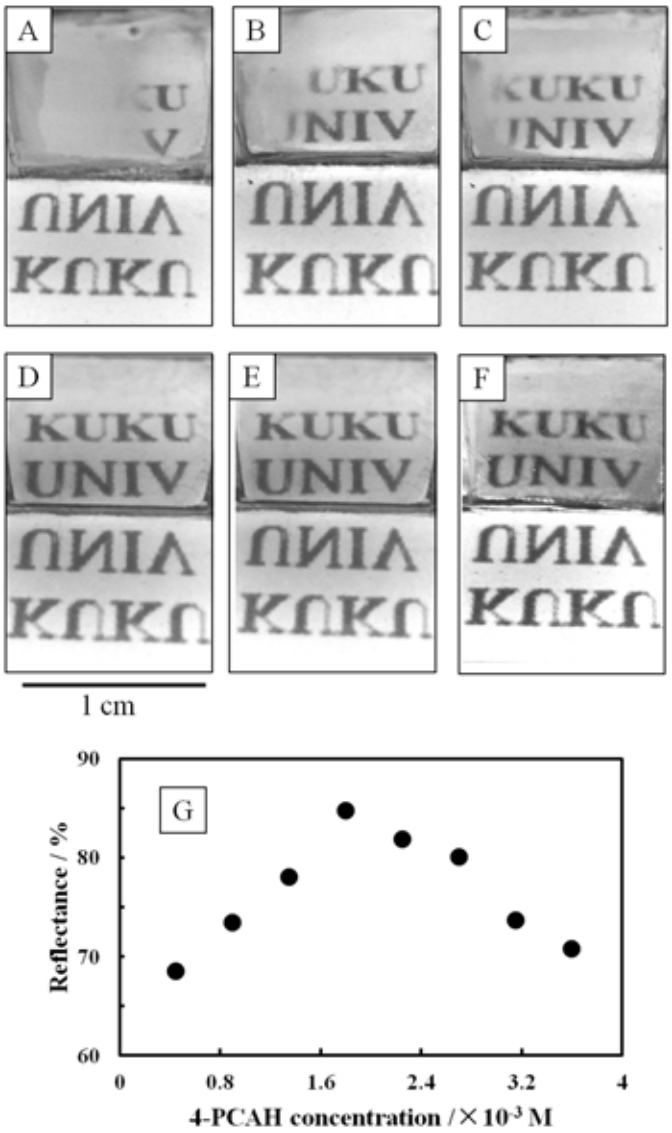

Figure 4. Micrographs (A-F) of Al film surfaces obtained by electrodeposition and dependence (G) of the reflectance of visible light (wavelength: 450 nm) on the 4-pyridinecarboxylic acid hydrazide concentration. The EMIC/$AlCl_3$/toluene composition was fixed at an EMIC-$AlCl_3$ molar ratio of 1:2 and 9.25 M toluene. The concentrations of 4-pyridinecarboxylic acid hydrazide were as follows: (A) 0.45, (B) 0.9, (C) 1.35, (D) 1.8, (E) 2.7 and (F) 3.6 mM. Deposition time: 2 h; constant current density: 8.0 $mA \cdot cm^{-2}$. The characters "KUKU UNIV" were reflected on the deposited Al (upper part: Al film, lower part: printed-out characters). Reprinted from Electrochim. Acta, 215, Uehara, K., Yamazaki, K., Gunji, T., Kaneko, S., Tanabe, T., Ohsaka, T. and Matsumoto, F., Evaluation of Key Factors for Preparing High Brightness Surfaces of Aluminum Films Electrodeposited from $AlCl_3$-1-Ethyl-3-Methylimidazolium Chloride-Organic Additive Baths, 556-565, Copyright (2016), with permission from Elsevier.

bath containing different concentrations (0.45-3.6 mM) of the 4-pyridinecarboxylic acid hydrazide additive [48]. A constant current density of 8.0 $mA \cdot cm^{-2}$ and a deposition time of 2 h were used for the entire Al electrodeposition process. To determine the brightness differences between the Al films, pictures were taken of the Al films on which the characters "KUKU UNIV" were reflected (upper part: Al film, lower part: printed-out characters). The visibility of the characters reflected on the Al films was considered a measure indicating the surface brightness. The reflectance increases from 69 to 78% when the 4-pyridinecarboxylic acid hydrazide concentration is increased from 0.45 to 1.35 mM, and it attains its maximum value (84%) at 1.8 mM. Further increasing the concentration leads to a gradual decrease in the reflectance.

Zhang *et al.* suggested the importance of electron density at the N atom of the pyridine ring of organic compounds as an additive to prepare bright Al coatings [83]. Bright Al coating could be electrodeposited with nicotinic acid and methyl nicotinate as additives, while lusterless Al coating was obtained in the presence of 3-methylpyridine, indicating that pyridine derivatives with electron-withdrawing groups could make the deposited Al surface brighter. When potential is applied to electrodes during the electrodeposition of Al films, the cathodic charge on the electrode surface is compensated in the first layer of cations. In this case, EMI^+ cations adsorb on the electrode surface. Additives also strongly adsorb on the electrode surface with EMI^+ cations (Figure 5). Strong adsorption of additives onto the surface of the growing Al nuclei hinders their further growth, producing very fine particles with sizes in the nanometer range and as a result Al films with high brightness. The adsorption point of the additives might be the N atom of the pyridine ring. The decrease in electron density at the N atom of the pyridine ring accelerates the adsorption of additives to the electrode surfaces. The degree of the electron drawing and electron donating ability of the functional groups that are connected to the pyridine ring by additive molecules determines the adsorption ability to the electrode surface. Their proposal can be accepted by other researchers. However, they compared the results obtained with only three additives. Additional results that follow their approach are needed. The addition of inorganic metal salts to

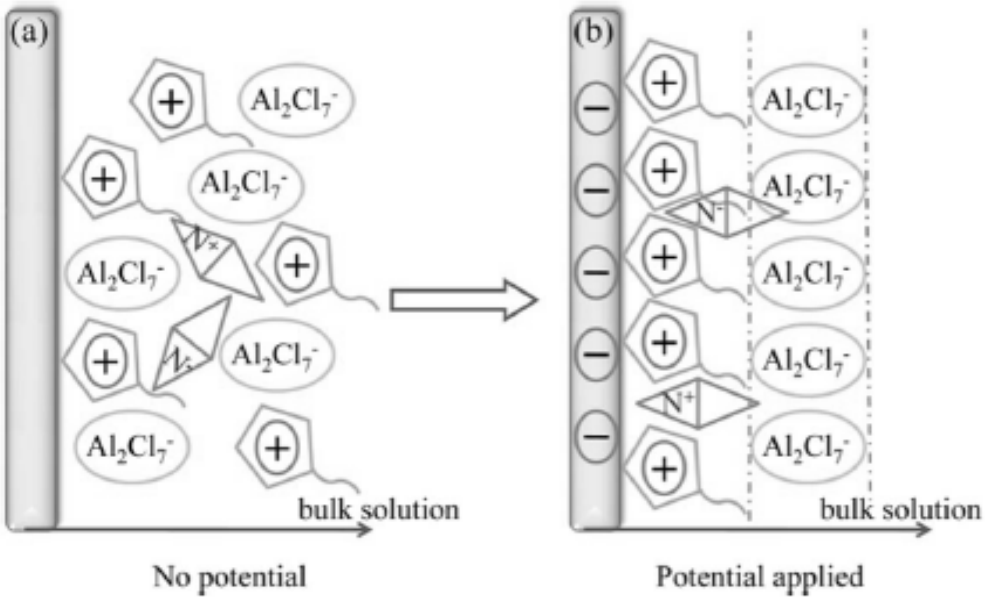

Figure 5. Schematic illustration of Al deposition with an organic additive containing N^+ from $AlCl_3$-EMIC ionic liquid. Reprinted with permission from J. Electrochem. Soc., 162 (8) D320 (2015). Copyright 2015, The Electrochemical Society.

the baths inhibits the crystal growth of Al deposits by adsorbing the species produced with inorganic metal salts to the deposit surfaces [92].

5. Electroless deposition of Al

Electroless deposition is one of the most important coating techniques and can produce even coatings on substrates with various shapes. If Al layers can be coated on many types of substrates by electroless deposition, high-corrosion-resistant layers can be applied on the substrates by Al. As far as we know, the first report on Al electroless deposition was published in 2008 by Koura and coworkers [93, 94]. After their studies, their idea was utilized in several applications for the formation of Al thin films [95-98]. For example, the Al precursor solution of $AlH_3\{O(C_4H_9)_2\}$ was prepared by an ethereal reaction of $AlCl_3$ with $LiAlH_4$ in $O(C_4H_9)_2$ [95]. The substrate on which the Al layer was to be deposited was treated with Ti(O-*i*-Pr)$_4$ to deposit TiO_x catalysts on the substrate. The treated substrate was immersed into the Al precursor solution of $AlH_3\{O(C_4H_9)_2\}$, and the decomposition of the Al precursor proceeded. The nucleation and grain growth of Al resulted in the formation of the Al layer on the substrate surface (Figure 6). In addition, the deposition of an Al layer with galvanic displacement of atoms on the substrates with Al atoms has been reported [99]. Several interesting papers on the electroless deposition of Al have been published. However, the kinds of solvent and reducing agent used in the process were limited. To spread the employment of electroless deposition of Al across many areas, water- and air-stable baths and reducing agents should be developed.

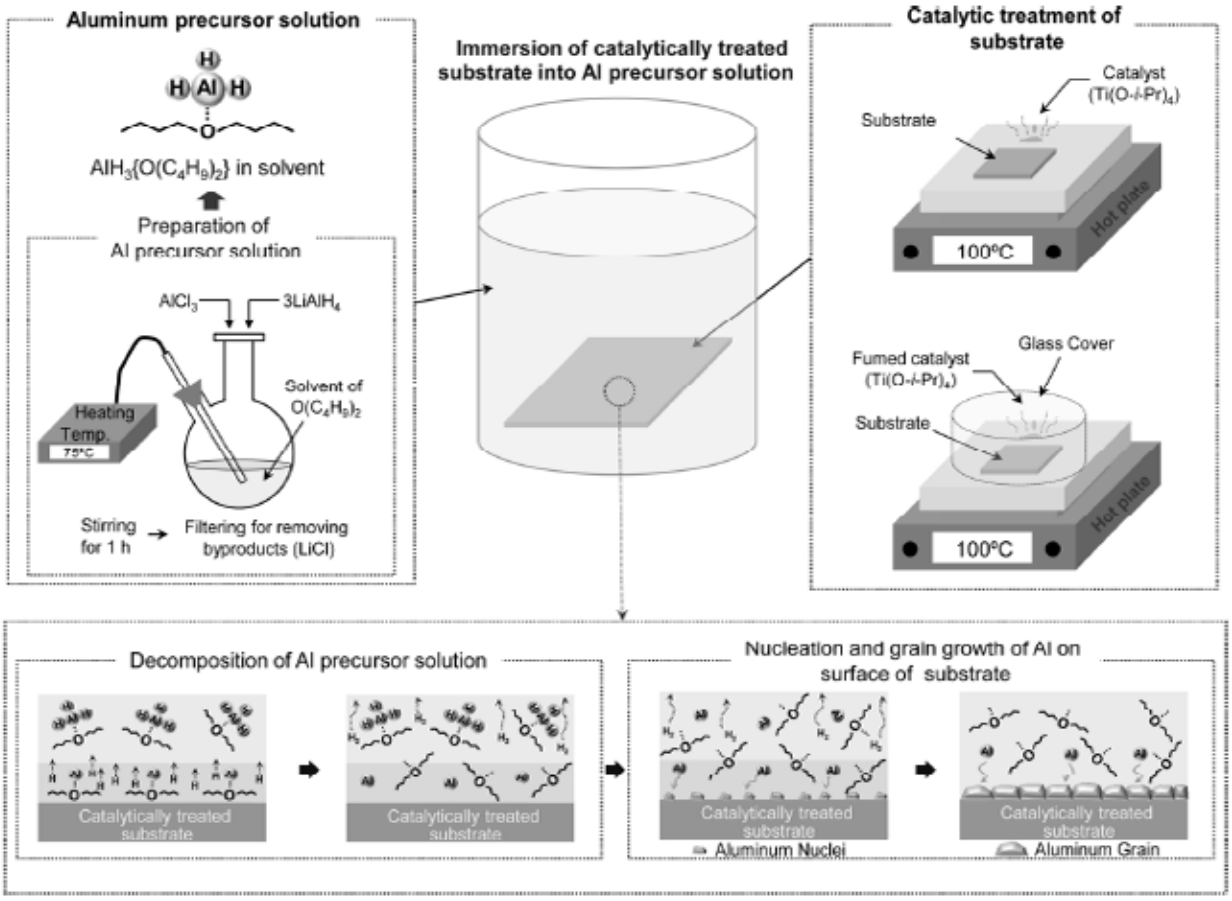

Figure 6. Schematic description of the process and mechanism of electroless Al deposition. Reprinted with permission from [95]. Copyright 2013 American Chemical Society.

Although not accurate, research on light-induced Al deposition has also been examined (Figure 7) [100]. The photogenerated electrons are generated on the n-side of the p-n junction by emitting lights to the p-n junction. The $Al_2Cl_7^-$ ions are reduced using the photogenerated electrons, and Al metal is deposited on the n-side of the p-n junction. The resistivity of the Al layer deposited was as low as 4×10^{-6} Ω·cm. The value was 1.5 times that of bulk Al. The Al layer was formed on Si substrates by electrochemical deposition from an $AlCl_3$-1-ethyl-3-methylimidazolium chloride IL. The resistivity of the Al layer deposited was in the high 10^{-6} Ω·cm range [100].

Recently, an interesting Al film formation process assisted by the catalytic action of Pt nanoparticles deposited on the substrates on which Al film was to be formed was also applied in the wiring in circuits fabricated on Si substrates [101]. The source of the Al layer was triethylamine alane (AlH_3NEt_3). The AlH_3NEt_3 suffered dehydrogenation reaction by the catalytic action of the Pt nanoparticles and then was reduced to Al metal as schematically drawn in Figure 8. The pattern on which the lines of Al layer were orderly arranged was successfully formed using this Al formation method on silicon substrates (Figure 9). Both line width of the Al layer and the spaces between the lines were 20 μm.

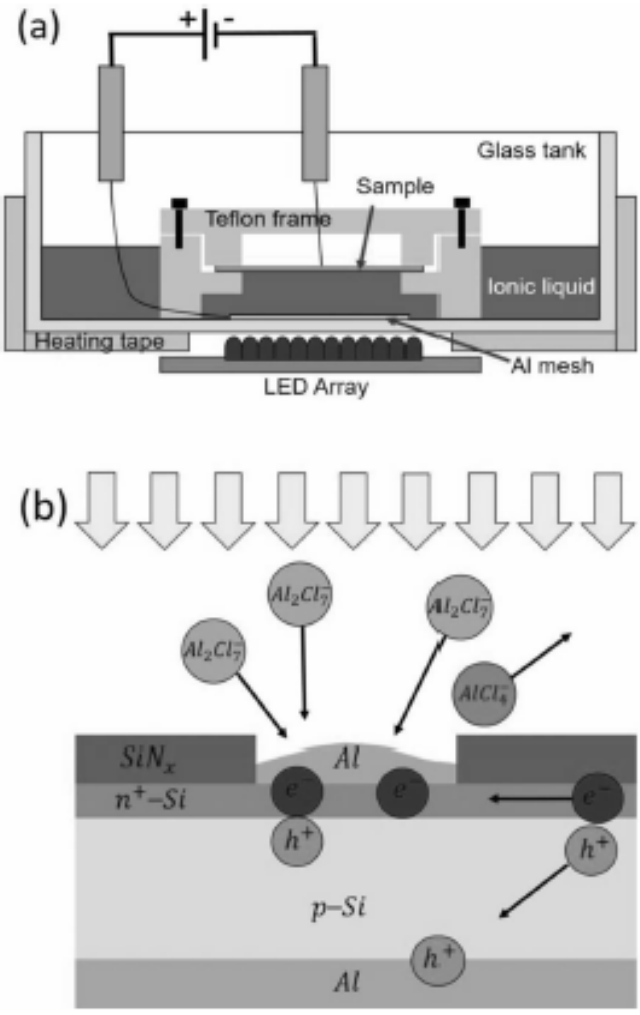

Figure 7. Schematic descriptions of (a) the experimental setup of light-induced Al deposition on p-Si and (b) the deposition mechanism. Reprinted with permission from J. Electrochem. Soc., 165, D381 (2018). Copyright 2018, The Electrochemical Society.

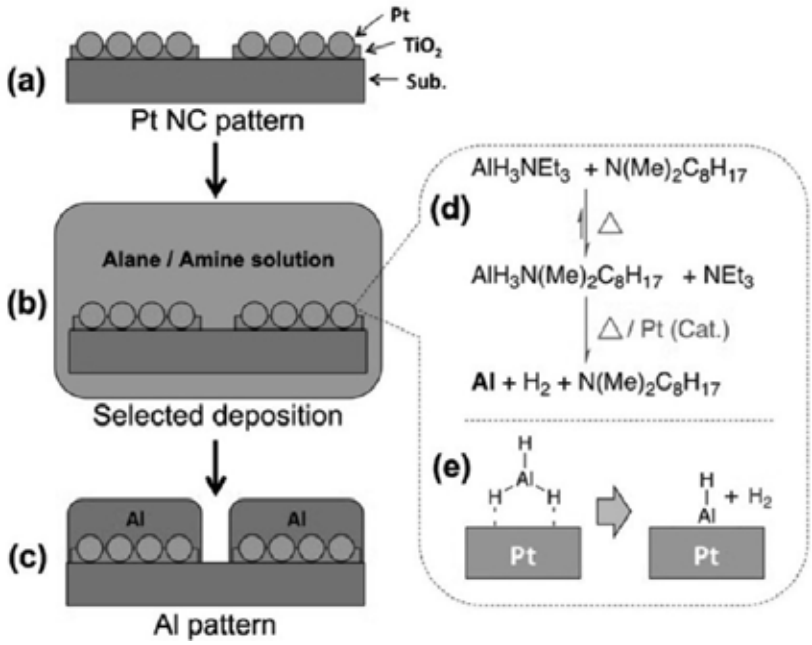

Figure 8. Schematic description of the catalytic deposition of Al on nanocrystalline Pt. (a) Formation of the Pt nanocrystalline pattern on Si substrate. (b) Immersing the substrate into alane solution at ~105-120 °C. (c) Al metal formation on the substrate. (d), (e) Reaction sequences for the formation of Al films. Reproduced with permission from [101], Copyright 2019 American Chemical Society.

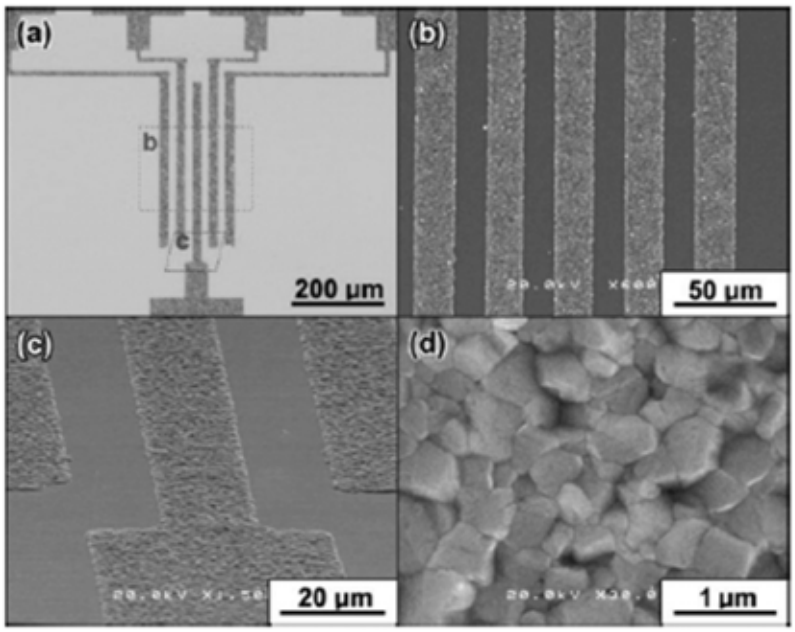

Figure 9. SEM images of Al layer deposited selectively on line pattern of copper on silicon substrate. (a) Optical microscopy of the 20 μm Al electrode pattern. (b) SEM image of the electrode pattern in the area marked with red lines in (a). (c) SEM image of the enlarged area marked with red lines in (a). (d) Highly magnified surface SEM image of Al film deposited on Si substrate. Reproduced with permission from [101]. Copyright 2012, American Chemical Society.

6. Micro- and nanofabrication with Al deposition

Al deposits of various shapes have been prepared using electrochemical deposition. The prepared deposits were used in many application areas to improve the reaction rate and the performance of devices. For preparing Al deposits of various shapes, there are two types of electrochemical deposition methods: methods using templates that support shape-formation of the nanostructures and methods that doesn't use the templates. When the templates are not used, the electrochemical parameters such as current density, deposition potential and presence/lack of stirring of the bath are the main factors for shape-formation.

In the case of "without the templates" methods, several instances of preparation of Al nano- and microwires and nanoparticles have been reported. The first interesting example of Al wire preparation was examined by Sun and coworkers using Lewis acidic $AlCl_3$/trimethylamine [102]. Fine nanowires with an average diameter of 222 nm and a length longer than 50 μm could be obtained on the W substrate surface (Figure 10). The length of the wires could be controlled using deposition time without significantly increasing the wire diameter. They suggested the contribution of a double layer structure to the formation of Al nanowires on electrode surfaces. The double layer appeared on the surface of electrodes when negative potential was applied to the electrode for Al deposition. The first layer of the double layer consists of the surface charge of ions adsorbed onto the electrode due to chemical interactions. The second layer is composed of ions attracted to the surface charge *via* the Coulomb force. These charges affect the mass-transfer of Al sources. Li and coworkers have also reported the electrochemical fabrication of Al nanowires using $AlCl_3$-1-butyl-1-methylpyrrolidinium chloride (BMPC) (mole ratio is 2:1) (Figure 11) [103]. They showed interesting SEM images of the electrochemical 2D nanofilm-3D nanonuclei-1D nanowire (EC 2D-3D-1D) growth of Al deposits from an $AlCl_3$/BMPC IL. Sun and coworkers proposed the mechanism of electrochemical growth of Ni–Zn alloy filament arrays from a basic $ZnCl_2$–EMIC ionic liquid containing $NiCl_2$ [104]. The electrochemical formation of Al wires from the $AlCl_3$/BMPC IL might also be controlled by the same mechanism. Electroactive species of $ZnCl_3^-$ ($Al_2Cl_7^-$ in the case of Al deposition) were consumed near the filament arrays (nanowire in the case of Al deposition), and the concentration of the less-active species of $ZnCl_4^{2-}$ ($AlCl_4^-$) increased around filaments because the reduction of $ZnCl_3^-$ ($Al_2Cl_7^-$) to Zn (Al) released Cl^- ions to the areas between the filaments (wires) (Zone II in reference [104]) (Figure 12).

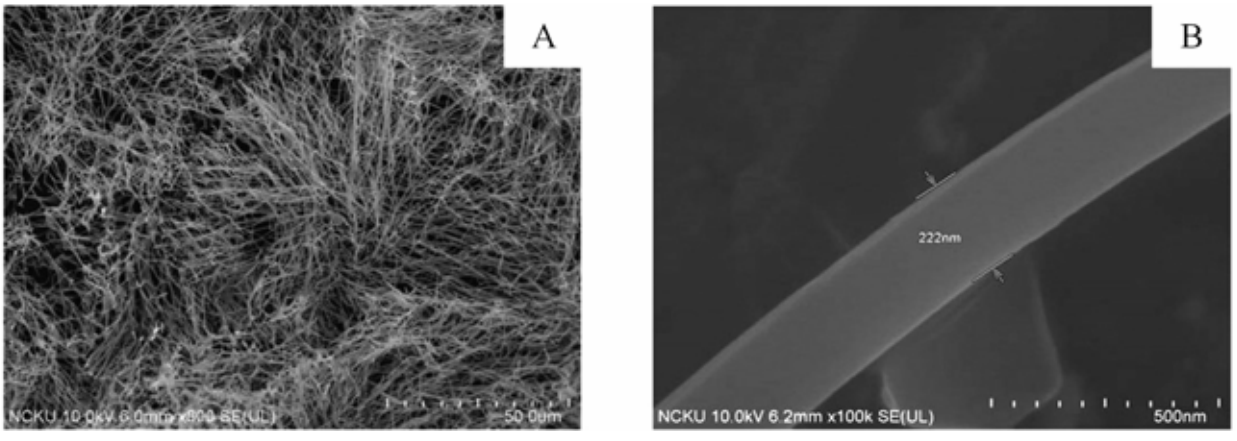

Figure 10. Low- and high-resolution SEM images of Al deposited electrochemically from Lewis acidic $AlCl_3$/trimethylamine hydrochloride ionic liquid. Reprinted from Electrochem. Commun., 34, Su, C.-J., Hsieh, Y.-T., Chen, C.-C., Sun, I.-W., Electrodeposition of aluminum wires from the Lewis acidic $AlCl_3$/trimethylamine hydrochloride ionic liquid without using a template, 170-173, Copyright (2013), with permission from Elsevier.

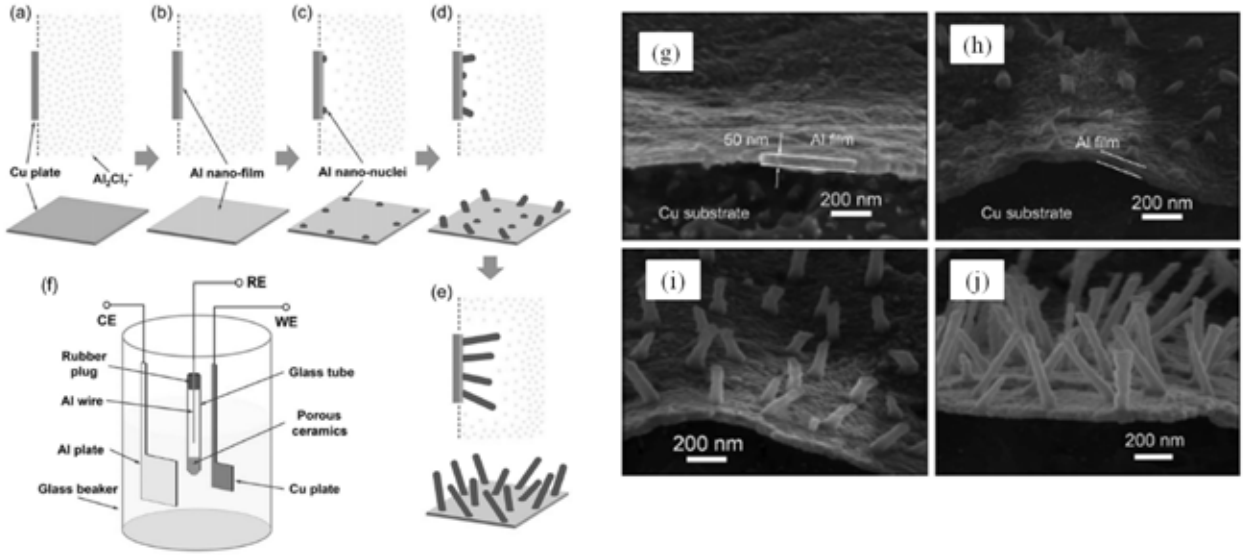

Figure 11. Schematic description of (a-e) electrochemical 3D-2D-1D Al deposit growth mechanism and experimental setup of electrochemical deposition and SEM images of Al deposited electrochemically from $AlCl_3$/1-butyl-1-methylpyrrolidinium chloride ionic liquid. (a) The partially peeled-off Al nano thin film, (b) the Al nano thin film with Al nanonuclei, (c, d) the Al nano thin film with Al nanowires. Reprinted with permission from J. Electrochem. Soc., 165, D641 (2018). Copyright 2018, The Electrochemical Society.

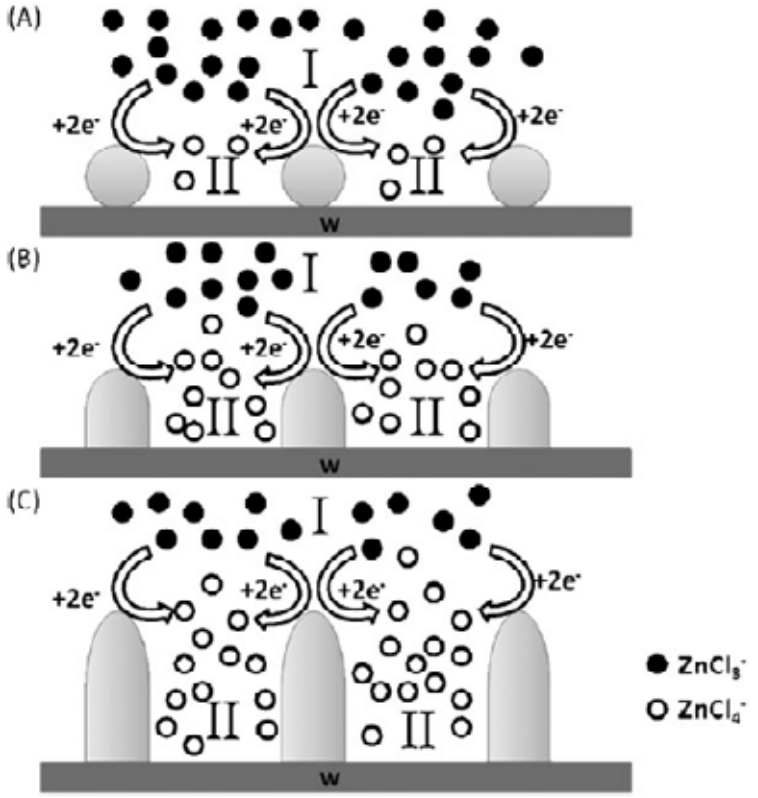

Figure 12. Schematic descriptions of the growth mechanism of the Ni-Zn filament array from a basic $ZnCl_2$–EMIC ionic liquid containing $NiCl_2$. Reproduced from [104] with permission from the Royal Society of Chemistry.

Nanoparticles are also one of the most important components for nanofabrication. Al nanoparticles react with water and generate heat and hydrogen gas. Therefore, the formation of Al nanoparticles has recently attracted much attention from many researchers and engineers [105]. The Al nanoparticles could be prepared by the electrochemical deposition of Al ions from ILs. Endres reported nanoparticle deposits of Al with $AlCl_3$-1-butyl-1-methyl pyrrolidinium bis(trifluoromethylsulfonyl)imide ILs for the first time [26]. In their next paper [28], SEM images of clear nanoparticles with deposit sizes less than 100 nm were reported (Figure 13). To obtain Al deposits in the nanoparticle form on an electrode surface, they changed the applied potential, substrates and deposition temperature. These conditions were carefully optimized to form Al nanoparticles on substrates. The preparation of Al nanoparticles was also tried using sonoelectrochemistry in which an ultrasound horn worked as a cathode and ultrasound emitter [106]. The sonoelectrochemistry was a new technique developed to prepare the nanoparticle form of metals, metal alloys, semiconductors and conducting polymers [107]. A solution of lithium aluminum hydride ($LiAlH_4$) and $AlCl_3$ in a tetrahydrofuran (THF) solvent was used. During Al deposition, current pulses and ultrasound pulses were applied to the solution. The short current pulse for depositing nanoparticles on substrates is immediately followed by a short ultrasound pulse for removing the deposited nanoparticles from the substrates. The average particle size of Al nanoparticles prepared using a sonoelectrochemistry system was 10-20 nm.

Nanorods and microporous structures could also be prepared by combining electrochemical deposition and templates. Al nanorods will be used for applications in optical measurements, such as

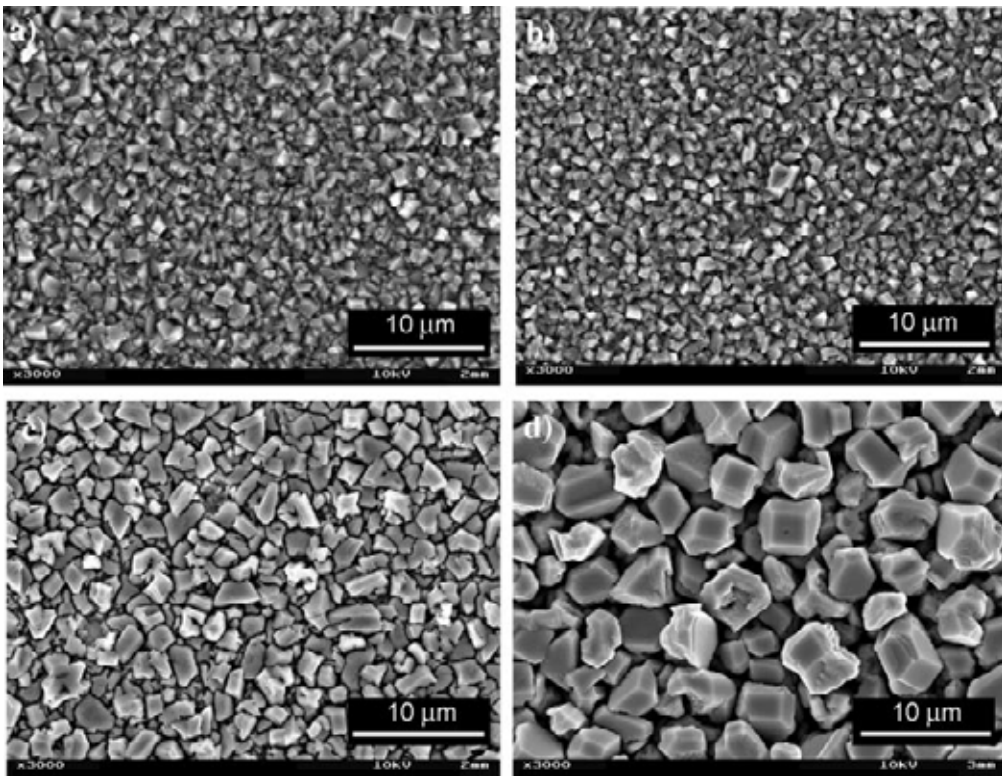

Figure 13. SEM images of electrochemical Al deposits on gold substrates from $AlCl_3$-1-butyl-1-methylpyrrolidinium-bis(trifluoromethylsulfonyl)imide with constant-potential electrolysis for 1 h at (a) -1.7 (room temperature), (b) -1.0 (50 °C), (c) -0.75 (75 °C) and (d) -0.45 (100 °C) V *vs.* Al/$AlCl_3$. Abedin, S. Z. E., Moustafa, E. M., Hempelmann, R., Natter, H. and Endres, F., 2006, ChemPhysChem, 7, 1535-1543. Copyright Wiley-VCH Verlag GmbH & Co. KGaA. Reproduced with permission.

surface plasmon resonance (SPR) [108]. For example, Pang reported the formation of Al nanorods using anodic porous alumina membranes (AAM) on which straight holes with diameters of 100 nm were arranged [109]. In the first step, Zn metal was filled in the holes of the AAM by electrochemical deposition. After that, Zn metal was replaced by Al metal by dipping the AAM/Zn into a solution containing 0.1 M $AlCl_3$ and 0.05 M EDTA and was buffered to pH = 7 with ammonia solution. The Al nanorods were obtained by dissolving the AAM with a mixed solution of phosphoric acid (6 wt%) and chromic acid (1.8 wt%). Nuclear track-etched polycarbonate membranes were also used as the template instead of AAM templates [110]. The UV-visible and FT-IR transmission spectra exhibited characteristics expected of Al nanorods [111]. In addition, macroporous Al films were synthesized using the template of hexagonally ordered three-dimensional structures formed using mono-sized polystyrene (PS) spheres and the electrochemical deposition of Al [112]. The gaps in the hexagonally ordered three-dimensional structures were filled with Al atoms. After chemical dissolution of the PS spheres, the macroporous Al films were synthesized. The macroporous Al films were used as a host material for Li deposition/stripping from/to ILs.

7. Application of Al deposition in the manufacture of batteries

Al batteries were recently researched by many researchers and engineers because it was reported that rechargeable Al-carbon batteries exhibited a relatively high discharge potential (~2 V), a specific capacity of 50-90 $mAh \cdot g^{-1}$ and a long cycle life of 7500 cycles [113, 114]. When the battery is charged, in the anode, $Al_2Cl_7^-$ ions are reduced to Al metal, as shown in eq. (1), and in the cathode, $AlCl_4^-$ ions (or $Al_2Cl_7^-$) are intercalated with graphite interlayers. In the discharging process, Al metal is oxidized to Al^{3+} ions, and the dissolved Al^{3+} ions react with $AlCl_4^-$ ions to form $Al_2Cl_7^-$ ions at the anode surface, and the $AlCl_4^-$ ions (or $Al_2Cl_7^-$) are deintercalated from graphite interlayers. The $AlCl_4^-$ ions (or $Al_2Cl_7^-$) are intercalated/ deintercalated in the charging/discharging process, similar to rocking-chair Li-ion batteries (Figure 14) [115]. The problems of cathode reactions for

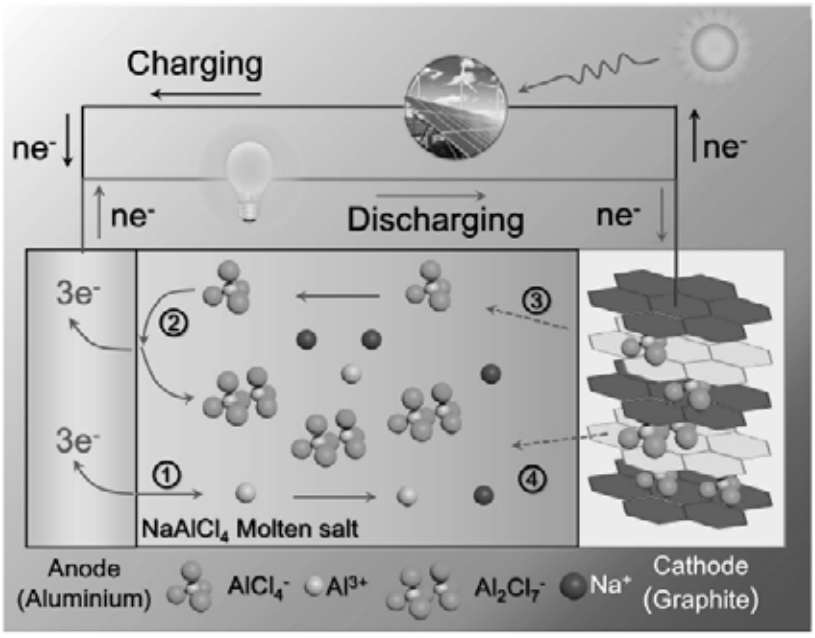

Figure 14. Schematic description of an Al-based full battery system. Discharging process: (1) Al metal is oxidized to Al^{3+} ions, (2) Al metal is oxidized to Al^{3+}, and upon Al^{3+} formation, $AlCl_4^-$ becomes to $Al_2Cl_7^-$, (3) $AlCl_4^-$ is deintercalated from the graphite interlayers, and (4) $Al_2Cl_7^-$ is deintercalated from graphite interlayers. Reproduced from [115] with permission from the Royal Society of Chemistry.

intercalation/deintercalation have been analyzed to improve the reaction efficiency [116]. Efforts have been made for improving cathode reactions of $AlCl_4^-$ ions (or $Al_2Cl_7^-$) by changing the cations in IL electrolytes [117]. The theoretical capacity of the Al anode is 2980 $mAh \cdot g^{-1,}$ which is comparable to 3860 $mAh \cdot g^{-1}$ observed for lithium [118]. In order to apply Al deposition/reduction reactions to secondary batteries, the capacity which Al potentially has should be obtained reversibly in the charging/discharging process of the batteries. Sun and coworkers examined the reversibility of the stripping/deposition of Al with various imidazolium cations and found that weak interactions between imidazolium cations and $Al_2Cl_7^-$ anions improved the reversibility of the stripping/deposition of Al [119]. An $AlCl_3$-1-methyl-3-propylimidazolium chloride (MPIM) IL exhibited the highest reversibility among DAIC. The battery produced using the $AlCl_3$-MPIM IL exhibited high discharging/charging efficiency compared with those using other ILs. 1-butyl-1-methylpyrrolidinium-bis(trifluoromethylsulfonyl) imide- and 1-ethyl-3-methylimidazolium-bis(trifluoromethylsulfonyl)imide-$AlCl_3$ ILs were compared from the perspective of reversibility of the stripping/deposition of Al. Although the ratio of anodic to cathodic charge for the stripping/deposition of Al is much lower, in the 1-butyl-1-methylpyrrolidinium-bis(trifluoromethylsulfonyl) imide-$AlCl_3$ IL, 1-ethyl-3-methylimidazolium-bis(trifluoromethylsulfonyl)imide-$AlCl_3$ IL exhibited a ratio close to 1 [28]. $AlCl_3$-triethylamine hydrochloride (Et_3NHCl) ILs ($AlCl_3/Et_3NHCl$ molar ratios = 1.0-1.7) have a Coulombic efficiency of stripping/deposition of Al of 95% and 91% for $AlCl_3$-EMIC ILs [120]. $AlCl_3$-LiCl-dimethylsulfone and $AlCl_3$ and urea in a 1.3:1 molar ratio also exhibited high Coulombic efficiency of stripping/deposition of Al [121, 122]. ILs of $AlCl_3$–NaCl–KCl at 393 K and $AlCl_3$–LiCl–KCl below 100 °C have also been reported to exhibit high reversibility for Al deposition/stripping [123, 124]. The $AlCl_3$–NaCl–KCl IL exhibited higher charging/discharging cycle performance for the deposition/stripping of Al than $AlCl_3$-EMIC IL [123]. The reversible Al deposition/stripping could be observed in gel polymer electrolytes in which $AlCl_3$-EMIC ILs were present at 80 wt% [125].

As in lithium batteries, in which Li metal is used as an anode, dendrite formation on anode surfaces after charging processes must be avoided to ensure safety of Al batteries. Al deposition also produces dendrites of Al metal in some cases [42], although Al has a low tendency towards dendrite growth [126]. In the case of Al deposition, there is discussion on the relationship between the structure of the electrical double layer in ILs and the surface morphology of the Al deposits. When the cathode is applied to the negative potential for Al deposition, imidazolium cations are adsorbed onto the cathode as the first layer, and a double layer is then formed on the cathode. The degree of penetration of $Al_2Cl_7^-$ active species into the double layer for Al deposition on the cathode surface depends on the structure of the double layer. When the $Al_2Cl_7^-$ active species cannot easily penetrate into the double layer, overpotential is needed, resulting in a larger grain size, rougher Al deposits, and ultimately Al dendrites [127]. Reddy *et al*. [42] examined the relationship between the substrates, overpotential and surface morphology of Al deposits. In their paper, based on the Volmer–Weber model, which considers the binding energy of the electrodeposited metal (M) either on the substrate (S), E_{MS}, or on the predeposited metal, E_{MM}, [128, 129], the surface modification of electrodes reduced the dendritic depositions of Al. Thus, the selection of substrates is important for inhibiting dendrite formation. For example, surfaces made of aluminum oxide, porous carbon paper and expanded graphite restricted the growth of crystalline Al dendrites due to a decrease in the nucleation sites and acceleration of the diffusion of active ions [130-132].

8. Conclusions

In this paper, we reviewed old and new materials and techniques for the electrochemical deposition of Al from anhydrous electrolytes. The problems that were identified at the early stage of electrochemical deposition of Al, such as ion conductivity, potential windows and moisture resistance, were overcome by developing new solvents, such as ILs and eutectic solvents. The applicability of Al deposition was also improved to near the point of practical trials. However, in all

research areas concerning Al deposition, the materials used to prepare the electrolytes are still very expensive. In addition, the durability of these recently developed materials has not been tested in mass production for long-term use. For Al deposition to be applied in mass production processes, the performance of these solvents should be examined and continually improved. If a mass production process for Al coating can be developed, there will be an abundance of Al products that are light and more noncorrosive.

ACKNOWLEDGEMENTS

This work was financially supported by the Light Metal Educational Foundation, Inc. in Japan.

CONFLICT OF INTEREST STATEMENT

There are no conflicts of interest.

REFERENCES

1. Wernick, S. and Pinner, R. 1956, Surface treatment and finishing of aluminum and its alloys, Robert Draper.
2. Haynes, W. M. 2010, CRC Handbook of Chemistry and Physics 91st Edition, CRC Press.
3. Chang, J.-K., Chen, S.-Y., Tsai, W.-T., Deng, M.-J. and Sun, I.-W. 2008, J. Electrochem. Soc., 155(3), C112-C116.
4. Sposito, G. 1989, The Environmental Chemistry of Aluminum, CRC Press.
5. Handbook of Deposition Technologies for Films and Coatings, 1994, 2nd Edition, Noyes Publications, Park Ridge, New Jersey.
6. Marder, A. R. 2000, Prog. Mater. Sci., 45(3), 191-271.
7. Wang, C. J. and Chen, S. M. 2011, Surf. & Coat. Tech., 206, 1277-1282.
8. Bard, A. J., Parsons, R. and Jordan, J. 1985, Standard Potentials in Aqueous Solution, Marcel Dekker Inc., New York, 566-567.
9. Simka, W., Puszczyk, D. and Nawrat, G. 2009, Electrochim. Acta, 54, 5307-5319.
10. Zhao, Y. and VanderNoot, T. J. 1997, Electrochim. Acta, 42, 3-13.
11. Chen, Q., Tan, D. Q., Liu, R. and Li, W. X. 2011, Surf. & Coat. Tech., 205, 4418-4424.
12. Grojtheim, K., Krohn, C., Malinovsky, M., Matiasovsky, K. and Thonstad, J. 1982, Aluminium Electrolysis Fundamentals of the Hall-Heroult Process, 2nd Ed., Aluminium-Verlag: Düsseldorf.
13. Couch, D. E. and Brenner, A. 1952, J. Electrochem. Soc., 99, 234-244.
14. Endres, F. 2002, Chemphyschem, 3, 144-154.
15. Plechkova, N. V. and Seddon, K. R. 2008, Chem. Soc. Rev., 37, 123-150.
16. Abbott, A. P., Harris, R. C., Hsieh, Y.-T., Ryder, K. S. and Sun, I. W. 2014, Phys. Chem. Chem. Phys., 16, 14675-14681.
17. Tsuda, T., Stafford, G. R. and Hussey, C. L. 2017, J. Electrochem. Soc., 164, H5007-H5017.
18. Zhang, Q., Wang, Q., Zhang, S., Lu, X. and Zhang, X. 2016, ChemPhysChem, 17, 335-351.
19. Giridhara, P., Abedin, S. Z. E. and Endres, F. 2012, Electrochim. Acta, 70, 210-214.
20. Sun, W.-C., Han, X. and Tao, M. 2015, ECS Electrochem. Lett., 4(4), D5-D7.
21. Choudhary, R. K., Kain, V. and Hubli, R. C. 2014, Surf. Engin., 30, 562-567.
22. Barchi, L., Bardi, U., Caporali, S., Fantini, M., Scrivani, A. and Scrivani, A. 2010, Prog. Org. Coat., 68, 120-125.
23. Hou, Y., Li, R. and Liang, J. 2018, Appl. Surf. Sci., 434, 918-921.
24. Abbott, A. P. and McKenzie, K. J. 2006, Phys. Chem. Chem. Phys., 8, 4265-4279.
25. Bakkar, A. and Neubert, V. 2015, Electrochem. Commun., 51, 113-116.
26. Abedin, S. Z. E., Moustafa, E. M., Hempelmann, R., Natter, H. and Endres, F. 2005, Electrochem. Commun., 7, 1111-1116.
27. Oriani, A. V., Cojocaruc, P., Monzani, C., Vallés, E. and Gómez, E. 2017, J. Electroanal. Chem., 793, 85-92.
28. Abedin, S. Z. E., Moustafa, E. M., Hempelmann, R., Natter, H. and Endres, F. 2006, ChemPhysChem, 7, 1535-1543.
29. Smith, E. L., Abbott, A. P. and Ryder, K. S. 2014, Chem. Rev., 114, 11060-11082.
30. Wilkes, J. S. 2002, Green Chem., 4, 73-80.

31. Paiva, A., Craveiro, R., Aroso, I., Martins, M., Reis, R. L. and Duarte, A. R. C. 2014, ACS Sustainable Chem. Eng., 2, 1063-1071.
32. Duruz, J. J. and Landolt, D. 1985, J. Appl. Electrochem., 15, 393-398.
33. Jafarian, M., Mahjani, M. G., Gobal, F. and Danaee, I. 2006, J. Appl. Electrochem., 36, 1169-1173.
34. Li, Q., Hjuler, H. A., Beng, R. W. and Bjerrum, N. J. 1990, J. Electgrochem. Soc., 137, 593-598.
35. Armand, M., Endres, F., MacFarlane, D. R., Ohno, H. and Scrosati, B. 2009, Nat. Mater., 8, 621-629.
36. Bonhôte, P., Dias, A.-P., Papageorgiou, N., Kalyanasundaram, K. and Grä1tzel, M. 1996, Inorg. Chem., 35, 1168-1178.
37. Abood, H. M. A., Abbott, A. P., Ballantyne, A. D. and Ryder, K. S. 2011, Chem. Commun., 47, 3523-3525.
38. Galiński, M., Lewandowski, A. and Stępniak, I. 2006, Electrochim. Acta, 51, 5567-5580.
39. Tang, J. and Azumi, K. 2011, Electrochim. Acta, 56, 1130-1137.
40. Chang, J.-K., Chen, S.-Y., Tsai, W.-T., Deng, M.-J. and Sun, I. W. 2007, Electrochem. Commun., 9, 1602-1606.
41. Ui, K., Yatsushiro, T., Futamura, M., Idemoto, Y. and Koura, N. 2004, J. Surf. Finish. Soc. Jpn., 55, 409-416.
42. Pradhan, D., Mantha, D. and Reddy, R. G. 2009, Electrochim. Acta, 54, 6661-6667.
43. Jiang, T., Brym, M. J. C., Dubé, G., Lasia, A. and Brisard, G. M. 2006, Surf. & Coat. Tech., 201, 1-9.
44. Li, B., Fan, C., Chen, Y., Lou, J. and Yan, L. 2011, Electrochim. Acta, 56, 5478-5482.
45. Abedin, S. Z. E., Giridhar, P., Schwab, P. and Endres, F. 2010, Electrochem. Commun., 12, 1084-1086.
46. Carlin, R. T., Crawford, W. and Bersch, M. 1992, J. Electrochem. Soc., 139(10), 2720-2727.
47. Liao, Q., Pitner, W. R., Stewart, G., Hussey, C. L. and Stafford, G. R. 1997, J. Electrochem. Soc., 144, 936-943.
48. Uehara, K., Yamazaki, K., Gunji, T., Kaneko, S., Tanabe, T., Ohsaka, T. and Matsumoto, F. 2016, Electrochim Acta, 215, 556-565.
49. Bakkar, A. and Neubert, V. 2013, Electrochim. Acta, 103, 211-218.
50. Tu, X., Zhang, J., Zhang, M., Cai, Y., Lang, H., Tian, G. and Wang, Y. 2017, RSC Adv., 7, 14790-14796.
51. Liu, Q. X., Abedin, S. Z. E. and Endres, F. 2008, J. Electrochem. Soc., 155, D357-D362.
52. Liao, Q., Pitner, W. R., Stewart, G., Hussey, C. L. and Stafford, G. R. 1997, J. Electrochem. Soc., 144, 936-943.
53. Takahashi, S., Koura, N., Kohara, S. and Saboungi, M.-L. 1999, Plasmas & Ions, 2, 91-105.
54. Kang, Y., Chen, S., Wang, Q., Lang, H., Jia, C. and Zhang, B. 2019, Ionics, 25, 163-169.
55. Abbott, A. P., Qiu, F., Abood, H. M. A., Aliac, M. R. and Ryder, K. S. 2010, Phys. Chem. Chem. Phys., 12, 1862-1872.
56. Endres, F. and Abedin, S. Z. E. 2006, Phys. Chem. Chem. Phys., 8, 2101-2116.
57. Hagiwara, R. and Ito, Y. 2000, J. Fluorine Chem., 105, 221-227.
58. Wilkes, J. S. and Zaworotko, M. J. 1992, J. Chem. Soc., Chem. Commun., 965-967.
59. Villagrán, C., Deetlefs, M., Pitner, W. R. and Hardacre, C. 2004, Anal. Chem., 76, 2118-2123.
60. Giridhar, P., Abedin, S. Z. E. and Endres, F. 2012, J. Solid State Electrochem., 16, 3487-3497.
61. Celik, Y. C., Pulletikurthi, G. and Endres, F. 2016, J. Solid State Electrochem., 20, 2781-2790.
62. Katayama, Y., Wakayama, T., Tachikawa, N., Yoshiii, K. and Serizawa, N. 2018, Electrochem., 86(2), 42-45.
63. Deng, M.-J., Chen, P.-Y., Leong, T.-I., Sun, I.-W., Chang, J.-K. and Tsai, W.-T. 2008, Electrochem. Commun., 10, 213-216.
64. Brown, L. C., Hogg, J. M. and Swadźba-Kwaśny, M. 2017, Top. Curr. Chem. (Z), 375, 78.

65. Galindo, M., Sebastian, P., Cojocaru, P. and Gomez, E. 2018, J. Electroanal. Chem., 820, 41-50.
66. Oriani, A. V., Cojocaru, P., Monzani, C., Vallés, E. and Gómez, E. 2017, J. Electroanal. Chem., 793, 85-92.
67. Zhang, Q., Vigier, K. D. O., Royer, S. and Jérôme, F. 2012, Chem. Soc. Rev., 41, 7108-7146.
68. Zhang, B., Shi, Z., Shen, L., Liu, A., Xu, J. and Hu, X. 2018, J. Electrochem. Soc., 165, D321-D327.
69. Li, M., Gao, B., Chen, W., Liu, C., Wang, Z., Shi, Z. and Hu, Z. 2015, Electrochim. Acta, 185, 148-155.
70. Li, M., Gao, B., Liu, C., Chen, W., Shi, Z., Hu, X. and Wang, Z. 2015, Electrochim. Acta, 180, 811-814.
71. Fang, Y., Jiang, X., Sun, X.-G. and Dai, S. 2015, Chem. Commun., 51, 13286-13289.
72. Fang, Y., Yoshii, K., Jiang, X., Sun, X.-G., Tusda, T., Mehio, N. and Dai, S. 2015, Electrochim. Acta, 160, 82-88.
73. Pulletikurthi, G., Bodecker, B., Borodin, A., Weidenfeller, B. and Endres, F. 2015, Prog. Nat. Sci. Mater. Inter., 25, 603-611.
74. Miyake, M., Kubo, Y. and Hirato, T. 2014, Electrochim. Acta, 120, 423-428.
75. Endo, A., Miyake, M. and Hirato, T. 2014, Electrochim. Acta, 137, 470-475.
76. Hu, P., Zhang, R., Meng, X., Liu, H., Xu, C. and Liu, Z. 2016, Inorg. Chem., 55, 2374-2380.
77. Mandai, T. and Johansson, P. 2016, J. Phys. Chem. C, 120, 21285-21292.
78. Jacquemin, J., Husson, P., Padua, A. A. H. and Majer, V. 2006, Green Chem., 8, 172-180.
79. Coleman, D. and Gathergood, N. 2010, Chem. Soc. Rev., 39, 600-637.
80. Ganapatibhotla, L. V. N. R., Zheng, J., Roy, D. and Krishnan, S. 2010, Chem. Mater., 22, 6347-6360.
81. Jiang, J., Zhao, W., Xu, Z., Li, Q., Yan, C. and Mu, T. 2016, ACS Sustainable Chem. Eng., 4, 5814-5819.
82. Wang, J., Wang, P., Wang, Q., Mou, H., Cao, H., Yu, D., Wang, D., Zhang, S. and Mu, T. 2018, ACS Sustainable Chem. Eng., 6, 15480-15486.
83. Wang, Q., Zhang, Q., Chen, B., Lu, X. and Zhang, S. 2015, J. Electrochem. Soc., 162(8) D320-D324.
84. Liu, L., Lu, X., Cai, Y., Zheng, Y. and Zhang, S. 2012, Aust. J. Chem., 65, 1523-1528.
85. Oniciu, L. and Muresan, L. 1991, J. Appl. Electrochem., 21, 565-574.
86. Tantavichet1, N. and Pritzker, M. D. 2005, Electrochim. Acta, 50, 1849-1861.
87. Oliveira, E. M., Finazzi, G. A. and Carlos, I. A. 2006, Surf. Coat. Technol., 200, 5978-5985.
88. Wang, Q., Chen, B., Zhang, Q., Lu, X. and Zhang, S. 2015, ChemElectroChem, 2, 1794-1798.
89. Zhang, Q., Wang, Q., Zhang, S. and Lu, X. 2014, J. Solid State Electrochem., 18, 257-267.
90. Miyake, M., Kubo, Y. and Hirato, T. 2014, Electrochim. Acta, 120, 423-428.
91. Endo, A., Miyake, M. and Hirato, T. 2014, Electrochim. Acta, 137, 470-475.
92. Shiomi, S., Miyake, M. and Hirato, T. 2012, J. Electrochem. Soc., 159, D225-D229.
93. Koura, N., Nagase, H., Sato, A., Kumakura, S., Takeuchi, K., Ui, K. and Loong, C. K. 2008, J. Electrochem. Soc. 155, D155-D157.
94. Shitanda, I., Sato, A., Itagaki, M., Watanabe, K. and Koura, N. 2009, Electrochim. Acta, 54, 5889-5893.
95. Lee, H. M., Choi, S.-Y. and Jung, A. 2013, ACS Appl. Mater. Interfaces, 5, 4581-4585.
96. Lee, H. M., Choi, S.-Y., Jung, A. and Ko, S. H. 2013, Angew. Chem. Int. Ed., 52, 7718-7723.
97. Poges, S., Jin, J., Guild, C., Li, W. N., Birnkrant, M. and Suib, S. L. 2018, Mater. Chem. Phys., 207, 303-308.
98. Lahiri, A., Pulletikurthi, G. and Endres, F. 2019, Frontiers in Chemistry, 7, 85.
99. Jiang, Y. D., Fang, L. P., Luo, L. Z., Wang, S. F. and Wang, X. L. 2018, J. Appl. Electrochem., 48, 827-834.
100. Wang, L., Huang, W.-H., Shin, W. J., Tao, W., Deng, B. and Wang, D. 2018, J. Electrochem. Soc., 165, D381-D383.

101. Shen, Z., Matsuki, Y. and Shimoda, T. 2012, J. Am. Chem. Soc., 134, 8034-8037.
102. Su, C.-J., Hsieh, Y.-T., Chen, C.-C. and Sun, I.-W. 2013, Electrochem. Commun., 34, 170-173.
103. Wang, H. and Li, B. 2018, J. Electrochem. Soc., 165, D641-D646.
104. Yang, J. M., Gou, S.-P. and Sun, I.-W. 2010, Chem. Commun., 46, 2686-2688.
105. Ghanta, S. R. and Muralidharan, K. 2013, J. Nanopart. Res., 15, 1715.
106. Mahendiran, C., Ganesan, R. and Gedanken, A. 2009, Eur. J. Inorg. Chem., 2050-2053.
107. Sáez, V. and Mason, T. J. 2009, Molecules, 14, 4284-4299.
108. Langhammer, C., Schwind, M., Kasemo, B. and Zorić, I. 2008, Nano Lett., 8, 1461-1471.
109. Pang, Y. T., Menga, G. W., Zhang, L. D., Shana, W. J., Zhang, C., Gao, X. Y. and Zhao, A. W. 2003, Solid State Sci, 5, 1063-1067.
110. Abedin, S. Z. E. and Endres, F. 2012, ChemPhysChem., 13, 250-255.
111. Pomfret, M. B., Brown, D. J., Epshteyn, A., Purdy, A. P. and Owrutsky, J. C. 2008, Chem. Mater., 20, 5945-5947.
112. Gasparotto, L. H. S., Prowald, A., Borisenko, N., Abedina, S. Z. E. A. and Endres, G. F. 2011, J. Power Sources, 196, 2879-2883.
113. Lin, M. C., Gong, M., Lu, B., Wu, Y., Wang, D. Y. and Guan, M. 2015, Nature, 520, 324-328.
114. Sun, H., Wang, W., Yu, Z., Yuan, Y., Wang, S. and Jiao, S. 2015, Chem. Commun., 51, 11892-11895.
115. Song, Y., Jiao, S., Tu, J., Wang, J., Liu, Y., Jian, H., Mao, X., Guo, Z. and Fray, D. J. 2017, J. Mater. Chem. A, 5, 1282-1291.
116. Hu, Y., Sun, D., Luo, B. and Wang, L. 2019, Energy Technol., 7, 86-106.
117. Zhu, G., Angell, M., Pan, C.-J., Lin, M.-C., Chen, H., Huang, C. J., Lin, J., Achazi, A. J., Kaghazchi, P., Hwang, B.-J. and Dai, H. 2019, RSC Adv., 9, 11322-11330.
118. Li, Q. and Bjerrum, N. J. 2002, J. Power Sources, 110, 1-10.
119. Yang, C., Wang, S., Zhang, X., Zhang, Q., Ma, W., Yu, S. and Sun, G. 2019, J. Phys. Chem. C, 123, 11522-11528.
120. Xu, H., Bai, T., Chen, H., Guo, F., Xi, J., Huang, T., Cai, S., Chu, X., Ling, J., Gao, W., Xu, Z. and Gao, C. 2019, Energy Storage Mater., 17, 38-45.
121. Legrand, L., Tranchant, A. and Messina, R. 1994, Electrochim. Acta, 39, 1427-1431.
122. Angell, M., Pan, C.-J., Rong, Y., Yuan, C., Lin, M.-C., Hwang, B.-J. and Dai, H. 2017, PNAS, 114, 834-839.
123. Chen, C.-Y., Tsuda, T., Kuwabata, S. and Hussey, C. L. 2018, Chem. Commun., 54, 4164-4167.
124. Wang, J., Zhang, X., Chu, W., Liu, S. and Yu, H. 2019, Chem. Commun., 55, 2138-2141.
125. Sun, X.-G., Fang, Y., Jiang, X., Yoshii, K., Tsuda, T. and Dai, S. 2016, Chem. Commun., 52, 292-295.
126. Jäckle, M., Helmbrecht, K., Smits, M., Stottmeister, D. and Groß, A. 2018, Energy Environ. Sci., 11, 3400-3407.
127. Zheng, Y., Zheng, Y., Peng, C., Zhao, Z. and Tian, D. 2016, Int. J. Electrochem. Sci., 11, 9585-9598.
128. Lorenz, W. J. and Staikov, G. 1995, Surf. Sci., 335, 32-43.
129. Budevski, E., Staikov, G. and Lorenz, W. J. 1996, Electrochemical Phase Formation and Growth, VCH Publications, New York.
130. Chen, H., Xu, H., Zheng, B., Wang, S., Huang, T., Guo, F., Gao, W. and Gao, C. 2017, ACS Appl. Mater. Interfaces, 9, 22628-22634.
131. Zhang, M., Watson, J. S., Counce, R. M., Trulove, P. C. and Zawodzinski Jr., T. A. 2014, J. Electrochem. Soc., 161, D163-D167.
132. Muñoz-Torrero, D., Leung, P., García-Quismondo, E., Ventosa, E., Anderson, M., Palma, J. and Marcilla, J. 2018, J. Power Sources, 374, 77-83.